General Correlation of the Initial Collection Efficiency of Granular Filter Beds

A general correlation for the prediction of the initial collection efficiency of granular filter beds is proposed. The correlation is based on the results obtained from trajectory calculation and the comparison between the numerical results and available experimental data. The correlation includes all the pertinent dimensionless groups and agrees with reported data within experimental accuracy.

HEMANT PENDSE and CHI TIEN

Department of Chemical Engineering and Materials Science
Syracuse University
Syracuse, NY 13210

SCOPE

The performance of a filter bed can be characterized by its collection efficiency. Deep bed filtration, by nature, is a transient process; accordingly, the collection efficiency and the pressure drop across the bed vary during the course of filtration. For aerosol filtration in granular beds, the collection efficiency is known to increase with time. The initial collection efficiency, therefore, in many cases, can be used to provide a conservative estimate in design calculations.

The initial collection efficiency can be estimated with the classical trajectory analysis. The filter bed is represented by an appropriate porous media model and viewed as an assembly of collectors. The rate of particle collection is considered in terms of the rate of deposition of particles on the surfaces of these collectors as the suspension flows past the collectors. Studies of this kind using Happel's model for filter bed representation have been made before, the results however were found to be an order of magnitude different from experimental data.

In the present work the problem of particle collection in granular media was studied with the use of the recently proposed constricted tube model. In contrast to Happel's model, the constricted tube model is of the internal flow type and is intrinsically more suitable for the study of deep bed filtration (Pendse et al., 1978). Three different types of tube configuration were used in the calculation of the initial collection efficiency.

The initial collection efficiency, η_0, was found to depend strongly on the configuration of the tube and the flow field expression which describes the flow inside the tube. By comparisons with experimental data, it was found that agreement between the results of trajectory calculation and experiment can be obtained if the collectors are represented by a combination of two different tube configurations. Furthermore it was found possible, based on the numerical results, obtained from trajectory calculation, to determine the effects of the various dimensionless groups on the collection efficiency. By using these two approaches a generalized correlation of η_0 incorporating all the relevant dimensionless groups was obtained.

CONCLUSIONS AND SIGNIFICANCE

A general correlation of the initial collection efficiency of granular filter beds was established. In contrast to earlier empirical correlations, this correlation is based on results obtained from trajectory calculation and includes all the pertinent dimensionless groups. Comparisons of the correlation with available experimental data indicate that it does not display bias (favorable or unfavorable) toward any particular set of data. Agreement within a factor of two to three was observed in most casts.

The trajectory calculation which provides the basis for the development of this general correlation also indicates that significantly different values of η_0 were obtained corresponding to different types of tube configuration. This is contrary to the results of pressure drop and convective mass transfer calculations (Pendse, 1979; Chiang and Tien, 1980). A primary reason of this behavior can be attributed to the effect of secondary gas flow on particle trajectories.

The performance of a filter can be described by its overall collection efficiency, E, defined as

$$E = 1 - \frac{c_{\text{eff}}}{c_{\text{in}}} \tag{1}$$

where c_{in} and c_{eff} are the particle concentrations of the influent and effluent streams respectively.

Although the overall collection efficiency, E, provides a direct indication of particulate removal capability, it is not a fundamental quantity which can be readily correlated with operating variables. Payatakes et al. (1973) suggested that granular filter bed can be considered to be composed of a number of unit bed elements (UBE) of thickness l, each of which, in turn, consists of a number of geometrically similar collectors (unit cells) (Figure 1). The particle collection capabilty of the filter bed therefore can be expressed in terms of the collection efficiency of the individual unit bed element. Let η_i denote the collection efficiency of the i-th unit bed element, by definition,

$$\eta_i = \frac{c_{i-1} - c_i}{c_{i-1}} \tag{2}$$

where c_i and c_{i-1} are the concentrations of fluid stream leaving the i-th and $(i-1)$th UBE respectively.

H. Pendse is presently with the Department of Chemical Engineering, University of Maine at Orono, Orono, Maine 04469.

0001-1541-82-4889-0677-$2.00.

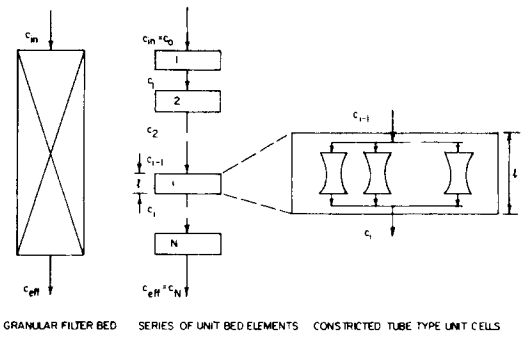

Figure 1. Schematic representation of a granular filter bed.

For a bed of height L, which is composed of N unit bed elements (i.e., $N = L/l$), the overall collection efficiency, E, becomes

$$E = 1 - \frac{c_{\text{eff}}}{c_{\text{in}}} = 1 - \frac{c_1}{c_{\text{in}}}\frac{c_2}{c_1}\cdots\frac{c_{\text{eff}}}{c_{N-1}}$$
$$= 1 - (1-\eta_1)(1-\eta_2)\ldots(1-\eta_N) \quad (3)$$

For a clean filter, $\eta_1 = \eta_2 = \ldots = \eta_0$, the above expression yields

$$E = 1 - (1-\eta_0)^{L/l}$$

or

$$\frac{c_{\text{eff}}}{c_{\text{in}}} = \exp\left(\frac{L}{l} ln\,(1-\eta_0)\right) \quad (4)$$

If one further assumes that the collectors contained in a unit bed element are identical in size and shape, the collection efficiency of the unit bed element and the collection efficiency of the individual collectors (known as the single collector efficiency) become the same. With the knowledge of the single collector efficiency, the performance of a filter can be predicted with the use of Eq. 4. (This, of course, is true if the filter remains clean, i.e., during the initial period of filtration.)

Most of the fundamental studies in deep bed filtration are concerned with the measurement and estimate of η_0. For the estimation of η_0, appropriate porous media model has to be chosen in order to specify the geometry of the collectors contained in the unit bed element and the flow field around the collectors. The single collector efficiency can then be estimated through trajectory calculation. Most of the previous studies belong to either one of the two categories; hydrosol filtration in granular bed and aerosol filtration in fibrous bed.

Relatively few basic studies have been made concerning aerosol filtration in granular media. Paretsky et al. (1971) calculated the initial collection efficiency of granular filter bed using the sphere-in-cell (Happel's model) model. Their calculated results however were found to differ significantly (by order of magnitude) from experimental data. An earlier work by the present authors (Pendse et al., 1978), in which the initial collection efficiency was calculated by assuming that the collector geometry is of the parabolic constricted tube type also yielded results substantially different from experiments. A more crude approximation of granular filter can be made with the use of the isolated collector model. Single collector efficiency estimated on such as basis has been reported by Tardos and coworkers (Tardos et al., 1976, 1978; Gutfinger and Tardos, 1979). Although reasonable agreement with experiment was claimed (Tardos et al., 1979), the predicted values differ from experiment by more than a factor of three in certain cases (Figures 5 and 6, Tardos et al., 1979). In addition to these theoretical calculations, a number of empirical correlations have also been proposed. These correlations are generally based on limited data and therefore do not incorporate all the dimensionless parameters relevant to particle deposition. The extension of any of these correlations beyond the conditions of the experimental data on which they are based is questionable.

The purpose of the present study is to present a general correlation of the initial collection efficiency, which can be used for design calculations. To provide the basis for this development, the initial collection efficiency was calculated using the constricted tube model for the representation of the filter media. Unlike the earlier work (Pendse et al., 1978), three different tube configurations were used. It was found possible to obtain good agreement between the calculated collection efficiency and experimental data if the collector geometry is assumed to be a combination of two types; parabolic constricted tube and sinusoidal constricted tube. Furthermore, the trajectory calculation results were used to obtain a more complete relationship between η_0 and the various dimensionless groups. The validity of the correlation was substantiated through its comparison with experimental data.

REPRESENTATION OF GRANULAR BED BY CONSTRICTED TUBE MODEL

With the use of the constricted tube model, the unit cells contained in a unit bed element are assumed to be of the shape of constricted tube. As an approximation, they are assumed to be uniform in size although more accurate representation would require them to be of a given size distribution (Payatakes et al., 1973). The model parameters are N_c, the number of constricted tubes per unit cross sectional area of the bed, l, the thickness of the unit bed element; h, the height of the unit cell, d_m the maximum diameter of the tube and d_c the constriction diameter of the tube. Table 1 summarizes the relationship between these parameters and the macroscopic filter bed properties.

A complete description of the constricted tube requires the specification of h, d_m, d_c, and the tube wall geometry. In the original formulation of Payatakes et al. (1973a), the wall geometry is assumed to be parabolic, i.e.

$$r_w(z) = r_1 + 4(r_2 - r_1)\left(0.5 - \frac{z}{h}\right)^2 \quad 0 \le \frac{z}{h} \le 1.0 \quad (5.a)$$

where r_1 and r_2 are the minimum and maximum radii; namely, $r_1 = d_c/2$ and $r_2 = d_m/2$.

Subsequently two other geometries have also been proposed; the sinusoidal geometry (Fedkiew and Newman, 1977) and the hyperbolic geometry (Venkatesan and Rajagopalan, 1980) which can be expressed as

Sinusoidal geometry

$$r_w(z) = \frac{r_1 + r_2}{2}\left[1 + \frac{r_2 - r_1}{r_2 + r_1}\cos\left(2\pi\frac{z}{h}\right)\right] \quad (5.b)$$

TABLE 1. DETERMINATION OF POROUS MEDIA MODEL PARAMETERS: CASE OF UNIFORM UNIT CELL SIZE

(1) Number of Constricted Tubes per Unit Area, N_c

$$N_c^* = N_c \cdot d_g^2 = \frac{6 \cdot \epsilon^{1/3}(1 - S_w)^{1/3} \cdot (1-\epsilon)^{2/3}}{\pi}$$

(2) Length of Unit Bed Element, l

$$l^* = \frac{l}{d_g} = \left[\frac{\pi}{6}\frac{1}{(1-\epsilon)}\right]^{1/3}$$

(3) Constriction Diameter, $d_c^\dagger$

$$d_c^* = \frac{d_c}{d_g} = 0.35 = 2r_1^* \text{ (Approximately)}$$

(4) Height of the Unit Cell, h

$$h = d_g$$

(5) Maximum Diameter of the Unit Cell, d_m

$$d_m^* = \frac{d_m^*}{d_g} = \left[\frac{\epsilon(1 - S_{wi})}{(1-\epsilon)}\right]^{1/3} = 2r_2^*$$

† d_c and S_{w_i} can be determined from capillary pressure-saturation data (Payatakes et al., 1973).

Hyperbolic geometry

$$r_w(z) = r_1\left[1 + \frac{\alpha^2 z^2}{h^2}\right]^{1/2}$$

$$\text{where } \alpha = 4\sinh^2\left[\cosh^{-1}\left(\frac{r_2}{r_1}\right)\right] \quad (5.c)$$

As shown in later sections, the use of different tube configurations lead to significantly different results in trajectory calculations.

The flow field within a constricted tube, of course, varies with the geometry of the tube and the degree of approximations introduced in obtaining the solution of the appropriate equations of motion. Three types of flow field expressions were used in the present study; the simplified flow field expression for all three types of tube geometry, the collocation solution of Neira & Payatakes (1978) for parabolic constricted tube and the perturbation solutions of Chow and Soda (1972). The simplified solution was obtained with the assumption that parabolic velocity profile is achieved along the axial distance. The stream function is given as:

$$\psi_0^* = \frac{\psi_0}{q} = \frac{1}{2\pi}\left[\left(\frac{r}{r_w}\right)^4 - \left(\frac{r}{r_w}\right)^2\right] \quad (6)$$

where q is the volumetric flow rate through the tube.

The collocation solution of Neira and Payatakes was obtained under creeping flow conditions. Accordingly it cannot be used to study the effect of fluid inertia. The perturbation solution is more general; it includes the inertia effect and is applicable to both types of tube geometries. In fact, the simplified flow field expression (i.e., Eq. 6) is the zeroth order solution of the perturbation solution.

ESTIMATION OF COLLECTION EFFICIENCY BY TRAJECTORY ANALYSIS

The principle of the trajectory analysis is illustrated in Figure 2. If the granular bed is represented by the constricted tube model, the retention of particles in the bed can be viewed as the deposition of particles on the surface of the tube through which the particle suspension flows. For any particle entering the tube, it may become collected or escape (i.e., flows out of the tube). In either case, the outcome can be determined by the trajectory of the particle. A particle may be considered as collected if its trajectory intercepts the tube wall (assuming that there is no bounce-off).

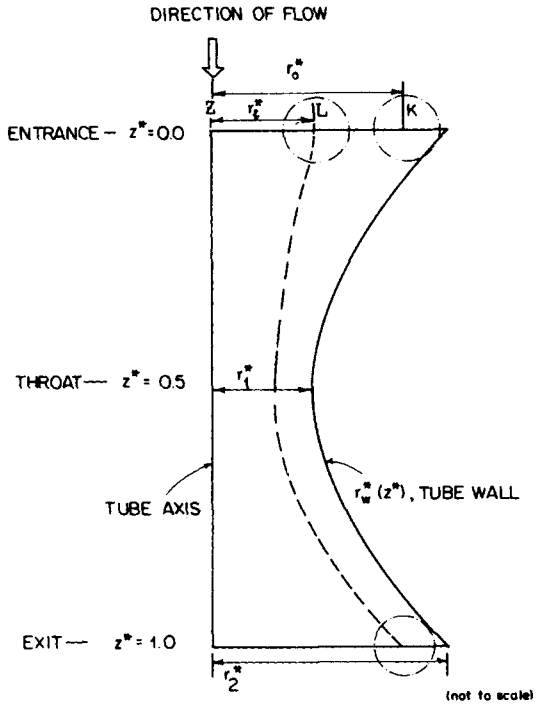

Figure 2. Schematic representation of limiting trajectory.

If the Brownian diffusion effect is unimportant, particle trajectories are deterministic. For particles entering the tube, their trajectories are uniquely determined by their initial positions at the inlet and different trajectories do not intersect one another. If one assumes that a particle which enters the tube at a radial position of $r^* = (r_1^*)$, (Point L, Figure 2) makes contact with the tube wall at its exit, it follows that all particles which are collected by the tube wall must have their initial positions between points L and K while those which escape must have initial positions between points Z and L. (As shown later, almost all the particles are deposited on the upper half of the tube. Accordingly, for practical purposes, the limiting trajectory can be considered to be the one which makes contact with the tube wall at its throat.) The trajectory beginning at point L is known as the limiting trajectory. The collection efficiency of the unit cell, $(\eta_0)_c$, defined as the fraction of particles entering the unit cell which become collected, is given as

$$(\eta_0)_c = \frac{\psi[0,r_l] - \psi[0,r_e]}{\psi[0,0] - \psi[0,r_e]} \quad (7)$$

where ψ is the stream function and r_e is the farthermost position that an entering particle may occupy. r_e is dependent upon the particle size and the shape of the tube wal and can be calculated readily from geometrical consideration for a given tube geometry and particle size.

If all the unit cells are of the same size, the collection efficiency of the unit bed element, in its clean state, η_0 becomes the same as $(\eta_0)_c$.

COLLECTION EFFICIENCY DUE TO INDIVIDUAL MECHANISMS

The mechanisms by which particle collection is effected are well known and include Brownian diffusion, interception, gravitation, inertial impaction and electrostatic effects. In many cases the collection efficiency due to the individual mechansims can be readily derived. These expressions can be used conveniently to assess the relative importance of the different mechanisms.

Rajagopalan and Tien (1976) obtained the following expressions for the collection efficiencies due to gravitation, Brownian diffusion and interception with the use of Happel's model.

$$(\eta_0)_G = (1-\epsilon)^{2/3} \cdot N_G \quad (8)$$

$$(\eta_0)_D = 4A_s^{1/3} N_{Pe}^{-2/3} \quad (9)$$

$$(\eta_0)_I = 1.5A_s(1-\epsilon)^{2/3} \cdot N_R^2 \quad (10)$$

where N_G,N_{Pe} and N_R are the gravitational, Peclet and relative size (interception) parameters, respectively. A_s is a parameter dependent upon the bed porosity, ϵ.

To obtain the expression of $(\eta_0)_I$, note that, in this case, particle trajectories coincide with fluid streamlines. From Eq. 7

$$(\eta_0)_I = \frac{\psi[0.5,(r_1^* - 0.5N_R)] - \psi[0,r_e^*]}{\psi[0,0] - \psi[0,r_e^*]} \quad (11)$$

A comparison of the calculated $(\eta_0)_I$ based on different flow fields corresponding to the three tube configurations was made. The results suggest that for all three configurations, the constricted tube model yields consistent values of $(\eta_0)_I$ for $N_R < 0.05$. Moreover, $(\eta_0)_I$ is insensitive to minor variations of flow field expressions. An analytical expression of $(\eta_0)_I$ can be found from Eq. 7 with the stream function given by Eq. 6 and the approximation $r_e^* = r_2^*$. The result is

$$(\eta_0)_I = N_R^2\left[\frac{4}{d_c^{*2}} - \frac{4N_R}{d_c^{*3}} - \frac{N_R^2}{d_c^{*4}}\right] \quad (12)$$

The above expression applies if the flow is creeping; namely $N_{Re,s} = 0$. The effect of fluid inertia on $(\eta_0)_I$ can be assessed by comparing the values of $(\eta_0)_I$ given by Eq. 12 and the corresponding values obtained with the stream function given by Chow and Soda (1972). This is shown in Figure 3 by plotting $(N_0)_{I,N_{Re,s}}/(N_0)_{I,N_{Re,s}=0}$ against $N_{Re,s}$. Also included in this figure is the combined collection efficiency due to inertial impaction and interception to be discussed

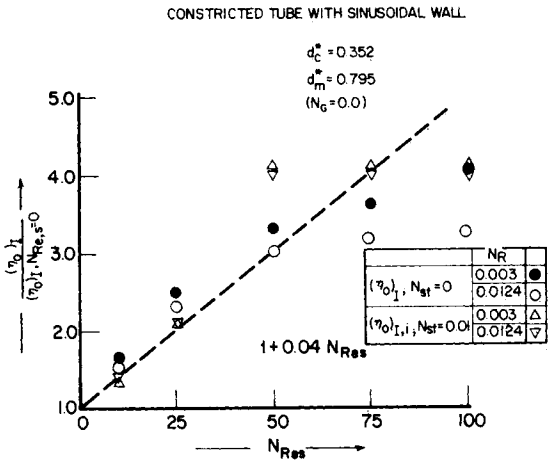

Figure 3. Effect of fluid inertia on initial collection efficiency.

later. For low Reynolds numbers, the fluid inertia effect can be represented as Pendse (1979).

$$\frac{(\eta_0)_I}{(\eta_0)_{2,N_{Re,s}=0}} = 1 + 0.04N_{Re,s} \tag{13}$$

CALCULATION OF COLLECTION EFFICIENCY WITH TRAJECTORY ANALYSIS

The deposition of aerosol particles in granular media, under most circumstances, is controlled by the effect of particle inertia. The particle trajectories, generally speaking, differ from fluid streamlines. The determination of the limiting trajectory (for the calculation of the collection efficiency) therefore has to be made from the integration of the equations of particle motion. The equations of particle motion are simply a consequence of the dynamic equilibrium of various forces. The forces considered in the present study are gravity, particle inertia and fluid drag. The force due to Brownian diffusion is excluded since it is relatively unimportant for particles of diameter greater than 2 m. Another notable exclusion is the electrical forces. This is not because they are unimportant, but because the study of the role of electrical forces in particle capture in itself can form a separate task.

The formulation of the equations of particle motion is based on the assumption that the particle concentration is sufficiently low so that the motion of one particle does not interfere with those of others. Furthermore, as a consequence of the axisymmetry of the fluid flow through the constricted tube, particle motion is assumed to be axisymmetric.

The force balance on a suspended particle along the z- and r-directions gives:

$$\frac{4}{3}\pi a_p^3\rho_p\frac{d^2z}{dt^2} = \frac{6\pi a_p\mu}{c_s}\left(v_z - \frac{dz}{dt}\right) + \frac{3}{4}\pi a_p^3(\rho_p - \rho_f)g \tag{14.a}$$

$$\frac{4}{3}\pi a_p^3\rho_p\frac{d^2r}{dt^2} = \frac{6\pi a_p\mu}{c_s}\left(v_r - \frac{dr}{dt}\right) \tag{14.b}$$

Equations 14.a and 14.b can be written into dimensionless form. First the following dimensionless variables are introduced.

$$z^* = z/h$$
$$r^* = r/h \tag{15}$$
$$t^* = \frac{tv_0}{h}$$

where h is the height of the unit cell and v_0 is the average velocity of fluid at the throat of the unit cell.

With the use of these variables, Equations 14.a and 14.b can be rewritten as follows:

$$\frac{d^2z^*}{dt^{*2}} = \frac{2}{N'_{St}}\left[\frac{v_r^*}{z} - \frac{dz^*}{dt^*} + N'_G\right] \tag{16.a}$$

$$\frac{d^2r^*}{dt^{*2}} = \frac{2}{N'_{St}}\left[v_r^* - \frac{dr^*}{dt^*}\right] \tag{16.b}$$

where

$$N'_{St} = \frac{4a_p^2\rho_p v_0 c_s}{9\mu h} \tag{17.a}$$

$$N'_G = \frac{2(\rho_p - \rho_f)ga_p^2c_s}{9\mu v_0} \tag{17.b}$$

v_z^* and v_r^* are the fluid velocity components normalized by v_0, and c_s is the Cunningham slip factor.

It is customary to express the inertia and gravity parameters in terms of the superficial velocity, V_s, and average grain diameter, d_g. For the constricted tube model with the assumption that all the tubes are of the same size, one has

$$h = d_g \tag{18}$$

$$v_0 = \frac{V_s}{N_c\left(\frac{\pi d_c^2}{4}\right)} \tag{19}$$

where N_c is the number of constricted tubes per unit cross-section of the bed, d_c is the constriction diameter and V_s is the superficial velocity.

Defining N_{St} and N_G as

$$N_{St} = \frac{4a_p^2V_s\rho_p c_s}{9\mu d_g} \tag{20}$$

and

$$N_G = \frac{2a_p^2(\rho_p - \rho_f)gc_s}{9\mu V_s} \tag{21}$$

one gets

$$N'_{St} = N_{St}\cdot\left(\frac{v_0}{V_s}\right) \tag{22}$$

$$N'_G = N_G\Big/\left(\frac{v_0}{V_s}\right) \tag{23}$$

As initial conditions for the solution of the equations of particle motion, the starting position of the particle is taken to be at the entrance of the tube, (z_0^*, r_0^*); and the initial velocity components are assumed to be

$$\left(\frac{dz^*}{dt^*}\right)_0 = v_{z,0}^* + \left(\frac{U_t}{v_0}\right) = v_{z,0}^* + N'_G \tag{24}$$

$$\left(\frac{dr^*}{dt^*}\right)_0 = v_{r,0}^* \tag{25}$$

where U_t is the terminal settling velocity of the suspended particle in unbounded fluid.

The purpose of the solution of trajectory equations is to determine the outcome of approaching particles as they move through the constricted tube. There are two possible outcomes. A particle may be collected by the tube wall or it may escape. The criteria used for this determination are:

1. A particle is assumed to be collected whenever at least one point of its trajectory satisfies the conditions

$$y = a_p \tag{26}$$

where y is the distance of the particle center from the tube wall. Notice that Eq. 26 has incorporated collection due to interception by accounting for the finite size of particles [i.e., the particle is assumed to be collected when the particle surface touches the tube wall].

2. If the particle trajectory exhibits a positive value of dy/dt before the condition of Eq. 26 is met, the particle is assumed to have escapted the unit cell. $(dy/dt) > 0$ indicates that the particle has gone past the point of its trajectory which corresponds to $y = y_{minimum}$ and moves away from the wall.

A trial and error procedure was used to determine the location of the limiting trajectory from which the collection efficiency can

be calculated. The procedure involved is as follows. Assume that the initial position of the limiting trajectory at the inlet of the constricted tube is $(0,r_1)$. Let the estimated value of r_1 be r_i in the i-th approximation and the corresponding interval of uncertainly be $2\Delta r_i$. In other words, r_1 belongs to the interval $(r_i - \Delta r_i, r_i + \Delta r_i)$. The particle trajectory corresponding to an initial position of $(0,r_i)$ can be obtained from the integration of the equations of particle motion [i.e. Eqs. 16.a and 16.b]. If the trajectory suggests the escape of the particle, r_1 must be between r_i and $(r_i + \Delta r_i)$ and a new estimate of r_1 can be taken to be $r_{i+1} = (r_i + \Delta r_i/2)$ and $\Delta r_{i+1} = \Delta r_i/2$. On the other hand, if the trajectory calculation indicates that the particle is collected, the next estimate of r_1 becomes $r_{i+1} = (r_i - \Delta r_i/2)$, and $\Delta r_{i+1} = \Delta r_i/2$. As the 1st approximation, one may take $r_1 = r_0/2$ and $\Delta r_1 = r_0/2$. In the present work, it was found that an estimate of r_1 which gives an accuracy of ±1% (for the collection efficiency) can be found with five to eight trials.

The numerical integrations were performed in double precision (accuracy up to 16 significant digits) using the fourth-order Runge-Kutta method. The time increment, (Δt^*) used was 0.01.A variable step algorithm was used to limit the relative change in either z- or r-coordinates in a single step within 1%.

TRAJECTORY CALCULATION RESULTS

Using the method presented before, computer runs were made to calculate the collection efficiency, η_0, for specified values of the dimensionless parameters, N_{St},N_R, $N_{Re,s}$ and N_G, corresponding to different tube geometries and flow field solutions. The major part of the calculations were made with $N_G = 0$ and $N_{Re,s} = 0$. The effect of gravitational force as stated before was found to be insignificant for small values of N_G, (see later discussions), while the effect of the fluid inertia can be approximately accounted for with the use of Eq. 13. The conditions used in the calculation are summarized in Table 2.

The results of the calculation are shown in Figure 4.a and 4.b. It is obvious that the calculated results are very sensitive to the tube geometry and the flow field expression used. This is particularly true for the predicted dependence of η_0 on the Stokes number, N_{St}. When the simplified flow expressions are used, the results indicate that η_0 decreases with the increase of N_{St} (curves BB and DD). Similar trends also exist if the tube geometry is assumed to be parabolic and the flow field is given by the perturbation solution (curve CC), although the decrease is much more gradual and the magnitude of the calculated collection efficiency predicted in this case is much greater than that based on the simplified flow field expression. For the same tube geometry (parabolic) but with the flow field expression given by the collocation solution, η_0 is found, at first, to decrease slowly with the increase of N_{St} until $N_{St} \approx 0.06$ and then increase abruptly (curve EE). By comparing curves EE and CC, it is also obvious that the flow field given by the perturbation solution predicts a significant inertial effect at relatively low Stokes number ($N_{St} = 0.001$) while the expression given by the collocation solution predicts no effect. At low N_{St}, curve EE approaches curve FF which represents the collection efficiency due to interception alone. On the other hand, an entirely different trend on the dependence of η_0 on N_{St} is observed if the tube geometry is assumed to be sinusoidal and the flow field expression is given by the perturbation solution (curve AA). In this case, η_0 is found to be a monotonically increasing function of N_{St}. At low value of N_{St}, curve AA is close to curve CC (parabolic geometry, perturbation solution) but at high values of N_{St}, it approaches curve EE (parabolic geometry, collocation solution). A comparison with experimental data suggests that curves AA and EE can be considered as the upper and lower bounds in the prediction of η_0. This point will be elaborated later.

The reason of this strong dependence on the tube geometry and various flow field solutions is not difficult to discern. The collection

TABLE 2. CONDITIONS USED IN TRAJECTORY CALCULATIONS SHOWN IN FIGURES 4.a. AND 4.b

Tube Dimensions:	$d_m^* = 0.795$, $d_c^* = 0.352$†
Tube Geometry:	Sinusoidal Wall, Parabolic Wall
Flow Field Expressions:	Perturbation Solution (Both Geometrics)
	Collocation Solution (Parabolic wall)
	Simplified Expression (Both Geometrics)
N_R	0.003, 0.0124
$N_{Re,s}$	0
N_G	0
N_{St}	0.001 to 1.0

† Corresponding to a granular bed with = 0.38.
A- A: Perturbation solution, sinusoidal wall
B-B: Simplified solution, sinusoidal wall
C-C: Perturbation solution, parabolic wall
D-D: Simplified solution, parabolic wall
E-E: Collocation solution, parabolic wall
F-F: Pure interception efficiency
G-G: Geometric mean of η-values based on (A-A) and (E-E)
H-H: $[N_{St} + (\eta)_{G\text{-}G}]$, Eq. 28
θ: Experimental data (Doganoglu, 1975)

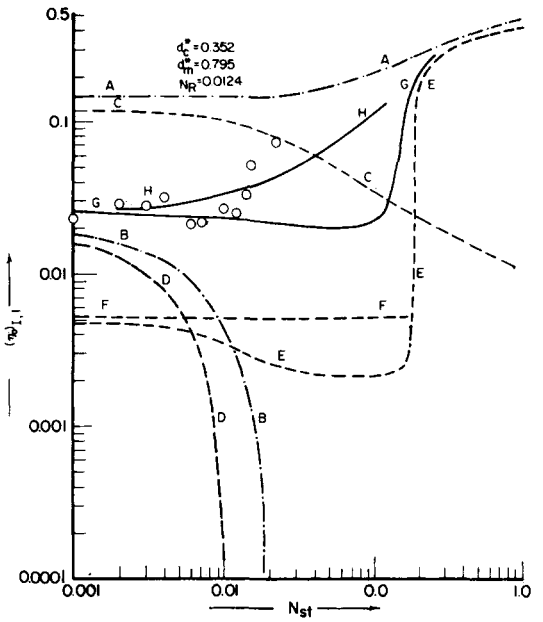

Figure 4a. Variation of (η_0) with N_{St},N_R = 0.0124.

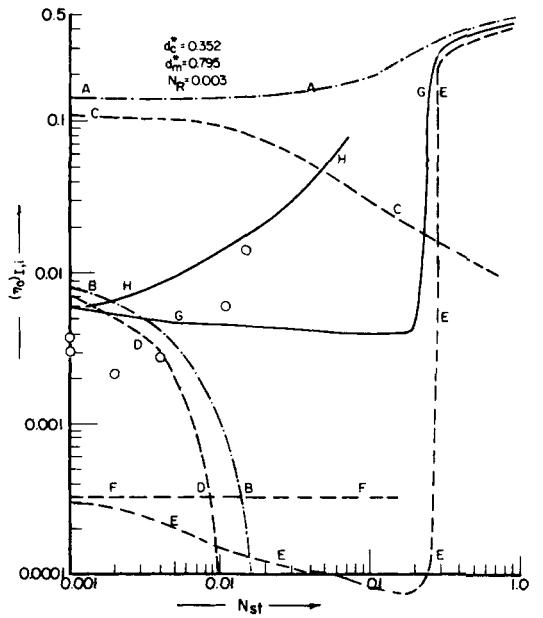

Figure 4b. Variation of (η_0) with N_{St},N_R = 0.003.

efficiency is influenced by the initial conditions used in the integration of the equations of particle motion and the local velocity of fluid near the entrance of the unit cell. Since the initial particle velocity is assumed to be that of the fluid, the orientation and placement of streamlines near the inlet of the unit cell becomes a critical factor. The simplified flow field expression (i.e., Eq. 6) predicts the streamlines near the tube wall at its entrance move along a direction away from the wall. A natural consequence of this is low collection efficiency. Furthermore, with such an orientation for the streamline, the collection efficiency will decrease as the particle inertia increases. This explains the behavior of curve BB and DD as shown in Figures 4.a and 4.b.

The use of a sinusoidal geometry and a more complete flow field expression implies that the streamlines at the entrance of the unit cell are parallel to the axial direction, and persist along that direction over a certain distance before they move toward the center. This is a much more favorable situation for particle collection, compared with the situation provided by the simplified flow field expression. As a result, the predicted value of η_0 is much higher. Greater particle inertia, which implies that a particle will more likely retain its initial direction along its flight, means greater liklihood for capture since the initial particle direction is oriented toward the wall. This explains that η_0 is found to be a monotonically increasing function of N_{St}.

The use of the parabolic geometry means that, at the entrance, the streamlines near the tube wall are necessarily oriented toward the center of the tube if no extraneous conditions (i.e., principle of periodicity) are imposed. Thus the use of the flow field expression given by the perturbation solution gives results which show a decrease of η_0 with the increase of N_{St} (curve CC). The flow field expression of the same geometry given by the collocation solution, on the other hand, was obtained with the use of the principle of periodicity. As a result, the streamlines at the entrance are parallel to the axis, but change their direction very quickly as they move into the cell. Accordingly, for lower N_{St}, the collection efficiency decreases with N_{St}. However, when the particle possesses sufficiently larger initial velocity, the inertial effect becomes dominant. This is shown by the large increase of η_0 with N_{St} and the fact that curve EE approaches curve AA at high N_{St}.

The disparate results shown in Figures 4.a and 4.b. raise a question; namely, for which one of the geometries and flow fields should the prediction of collection efficiency be used? To provide some insight, a comparison between the experimental data of Doganoglu (1975) and these predictions is made. Doganoglu's data, corrected for the gravitational and fluid inertia effects, are compared with the predictions (Figures 4.a and 4.b). These comparisons indicate that the data disagree with any single set of predictions. Instead the experimental data are found to be within the range of the predicted values. This leads to the natural and perhaps not too suprising conclusion that not a single geometry and flow field expression provide sufficiently accurate description for the study of particle deposition where the inertial effect is important. A combination of the various cases, namely by considering the unit cells to be of different geometries, may provide a practical solution to this problem. For example, if the geometrical mean of the values given by curves AA and EE is considered, the resulting curve, GG, gives a much better agreement with the data. Further improvement of such an approximation can be made to account for the expected dependence of η_0 on N_{St}. Since the results given by the two AA curves (Figures 4.a. and 4.b) can be approximated within the range of the Stokes number, $10^{-3} < N_{St} < 0.2$, by the expression

$$\eta_0 = \text{constant} + N_{St}, \tag{27}$$

one may conclude that η_0 can be given as

$$\eta_0 = N_{St} + (\eta_0)_{G-G} = N_{St} + \sqrt{(\eta_0)_{AA} \cdot (\eta_0)_{EE}} \tag{28}$$

which is shown by curve HH. Equation 28 provides the basis for the development of a correlation of η_0 to be discussed in the following section.

AVAILABLE EXPERIMENTAL DATA AND CORRELATIONS

The experimental data used are those reported by Knettig and Beeckmans (1974a), Doganoglu (1975), and Melcher et al. (1978). All of these data were obtained under conditions where the dominant mechanism of collection was inertial impaction. The data of Doganoglu and those of Melcher et. al. were obtained using liquid aerosols; thus the possible effect due to deposited particles was negligible. Knettig and Beeckmans' data were obtained over a relatively short period of filtration so that the collection efficiency they obtained can be considered to be that of the initial period. The conditions of these experiments are tabluated in Table 3. Summaries of these data can be found in Pendse's dissertation (1979).

A number of other investigators have also reported data on collection efficiency of granular filter bed when the inertial effect is dominant (Paretsky et al., 1971; Meisen and Mathur, 1974; Thambimuthu et al., 1978; Tardos et al., 1979). Unfortunately, these data were reported with incomplete information or only graphically and therefore cannot be used in this work. The correlations developed on the basis of these data, however, are included in the subsequent comparisons.

There exist several correlations established by previous investigators for the estimation of the collection efficiency of granular bed. These correlations are either for the total collection efficiency or collection efficiency due to one (inertial impaction) or two (inertial impaction and gravitation) mechanisms. They are as follows:

(i) Correlation by Paretsky (1972) [quoted in Doganoglu (1975)]

$$(\eta_0)_i = 2.0 N_{St}^{1.13} \tag{29}$$

(ii) Correlation by Meisen and Mathur (1974)

$$(\eta_0)i = 0.00075 + 2.6 N_{St} \tag{30}$$

(iii) Correlation by Knettig and Beeckmans (1974b)

$$(\eta_0) = 3.76 \cdot 10^{-3} - 0.454 N_{St} + 9.68 N_{St}^2 - 16.2 N_{St}^3 \quad \text{for} \quad N_{St} > 0.0416 \tag{31}$$

(iv) Correlation by Meltcher et al. (1978)

$$(\eta_0)_i = \beta N_{St} \tag{32.a}$$

where the dependence of β on $N_{Re,s}$ for $N_{Re,s} < 100$ may be expressed as:

TABLE 3. SUMMARY OF EXPERIMENTAL CONDITIONS

Investigator	Doganoglu (1975)	Knettig and Beeckmans (1974a)	Melcher et al. (1978)
Granular Medium	Glass Beads	Glass Beads	Glass Beads
Aerosol Particles	DOP (dioctylphthalate)	Uranine and Methylene blue (1:2 Wt Ratio)	DOP (dioctylphthalate)
Particle Diameter	1.35, 1.75 μm	0.8 – 2.9 μm	1.5 – 4 μm
Grain Diameter	110, 600 μm	425 μm	500 – 400 μm
Flow Direction	Downflow	Upflow	Downflow
Serial Numbers of Data Listed in Tables 7 to 9	19 through 54	1 through 18	55 through 60
Symbols Used in Figures 5 to 10	0	X	Δ

$$\beta = \begin{cases} 1.0 & \ldots N_{\mathrm{Re},s} < 100 \\ 0.01 N_{\mathrm{Re},s} & \ldots 100 > N_{\mathrm{Re},s} < 1{,}000 \\ 10 & \ldots\ldots\ldots N_{\mathrm{Re},s} > 1{,}000 \end{cases} \quad (32.b)$$

(v) Correlation by Doganoglu (1975)

$$(\eta_0)_{G,i} = 2.89 N_{\mathrm{St}} + 6.89 N_G \text{ for small grains } d_g = 100\ \mu\mathrm{m} \quad (33)$$

and

$$(\eta_0)_{G,i} = 0.0583 N_{\mathrm{Re},s} N_{\mathrm{St}} + 1.42 N_G \text{ for large grains } d_g = 600\ \mu\mathrm{m} \quad (34)$$

(vi) Correlation by Thambimuthu et al. (1978)

$$(\eta_0)_i = 10^5 \cdot N_{\mathrm{St}}{}^3 \quad \text{for } 10^{-3} < N_{\mathrm{St}} < 10^{-2} \quad (35)$$

Most of the correlations were developed with the investigator's own data and their differences are quite significant. Some of these differences undoubtedly are due to the widely different conditions used to obtain the data. For example, the correlation of Meltcher et al. (1978) is based on data of high Reynolds number [$10 < N_{\mathrm{Re},s} < 640$] while most of the other correlations are based on results corresponding to small $N_{\mathrm{Re},s}$ [$N_{\mathrm{Re},s} \ll 10$]. The expression of Meisen and Mathur (1974) was based on spouted bed data with the assumption that the annular region of a spouted bed is in the incipent stage of fluidization (i.e., about to be fluidized). Since these expressions are based on limited data, the incorporation of all the relevant dimensionless parameters was not possible.

PROCEDURE FOR DEVELOPING CORRELATION

The proposed correlation is established with the following premises:

(i) The dominant mechanism of collection is by inertial impaction and interception. The contributions by other mechanisms such as gravitation and Brownian diffusion are secondary. The total collection can be approximated by the addition of the individual contributions. [This assumption of additivity is incorrect in the strict sense as pointed out by Loffler (1979). However when the inertial impaction is the dominant mechanism, the use of this assumption should not introduce any significant error.]

(ii) The effect of fluid inertia on the collection efficiency due to inertial impaction and interception revealed by trajectory calculation is assumed to be valid. Consequently one may use Eq. 13 to account for the effect of fluid inertia.

(iii) Equation 28 is used to estimate $[(\eta_0)_{I,i}]_{N_{\mathrm{Re},s}=0}$. This is based on the findings of trajectory calculations, as shown in Figure 4.a and 4.b; namely a combination of unit cell geometries, provides a good description for granular media, or

$$[(\eta_0)_{I,i}]_{N_{\mathrm{Re},s}=0} = N_{\mathrm{St}} + \left[\{(\eta_0)_{I,i}\}_{P,N_{\mathrm{Re},s}=0} \cdot \{(\eta_0)_{I,i}\}_{s,N_{\mathrm{Re},s}=0}\right]^{1/2} \quad (36)$$

where the subscripts p and s refer to the parabolic geometry (collocation solution for flow field) and sinusoidal geometry (perturbation solution for the flow field) and the respective collection efficiencies are at $N_{\mathrm{Re},s} = 0$ and $N_{\mathrm{St}} = 0.001$ such that the collection efficiency is independent of N_{St}.

The results of Figures 4.a and 4.b suggest that, with the use of the parabolic tube geometry and with the flow field given by the collocation solution (i.e., curve EE) and at small values of N_{St}, $[(\eta_0)_{I,i}]_p$ is a function of N_R only and is close to $[(\eta_0)_I]_p$. Furthermore, from the simplified flow expression, $[(\eta_0)_I]_p$ is given by Eq. 12, or

$$[(\eta_0)_{I,i}]_{p N_{\mathrm{Re},s}=0} = N_R^2 \cdot \left\{\frac{4}{d_c^{*2}} - \frac{4N_R}{d_c^{*3}} - \frac{N_R^2}{d_c^{*4}}\right\} \quad (11)$$

To obtain an expression for $[(\eta_0)_{I,i}]_{s N_{\mathrm{Re},s}=0}$ values of $(\eta_0)_{I,i}$ were obtained using the sinusoidal geometry and flow field expression based on the perturbation solution for $N_{\mathrm{St}} = 0.001$ and various values of N_R. The results can be fitted into the following expression (Pendse, 1979)

$$[(\eta_0)_{I,i}]_{s N_{\mathrm{Re},s}=0} = 0.2302 N_R^{0.08243} \quad (37)$$

By combining Eqs. 36, 11 and 37, the final correlation is established as follows

$$(\eta_0)_{I,i} = (1 + 0.04 N_{\mathrm{Re},s}) \cdot \left[N_{\mathrm{St}} + \left\{0.48 \left(4 - \frac{4N_R}{d_c^*} - \frac{N_R^2}{d_c^{*2}}\right)^{1/2} \cdot \left(\frac{N_R^{1.041215}}{d_c^*}\right)\right\}\right] \quad (38)$$

COMPARISONS WITH EXPERIMENTAL DATA AND OTHER CORRELATIONS

The value of the generalized correlation proposed in the preceding section can be assessed by comparing its agreement with experimental data with those of other correlations. For this purpose, it is imporant that the experimental data be corrected to conditions similar to those values for the correlations. For example, Eq. 38 is for inertial impaction and interception. Equations 33 and 38 are for inertial impaction and gravitation. The other correlations mentioned earlier are for inertial impaction only.

The corrected experimental values used for comparison are

$$(\eta_0)_{\mathrm{expt},i} = (\eta_0)_{\mathrm{expt}} - [(\eta_0)_I + (\eta_0)_D + (\eta_0)_G] \quad (39)$$

$$(\eta_0)_{\mathrm{expt},I,i} = (\eta_0)_{\mathrm{expt}} - [(\eta_0)_D + (\eta_0)_G] \quad (40)$$

$$(\eta_0)_{\mathrm{expt},G,i} = (\eta_0)_{\mathrm{expt}} - (\eta_0)_D - (\eta_0)_I \quad (41)$$

The contributions due to the various individual mechanisms can be estimated from Eqs. 8–10. Details of the corrections are given elsewhere (Pendse, 1979).

The results of comparisons are shown in Figures 5–10 in which the ratio of the predicted collection efficiency, $(\eta_0)_{\mathrm{predicted}}$ to the experimental value, $(\eta_0)_{\mathrm{expt}}$ is plotted against $(\eta_0)_{\mathrm{exp}}$. The scattering of the data points around the horizontal line $(\eta_0)_{\mathrm{predicted}}/(\eta_0)_{\mathrm{exp}} = 1$ gives the accuracy of the correlation. The superiority of Eq. 38 over the correlations given by Paretsky, Meisen and Mather, Melcher et al. and Thambimuthu et al. is self-evident.

In comparing Eq. 38 with the correlations of Doganoglu, on the surface it may appear that the new correlation does not offer any significant improvement. There are, however, significant differences. First, Doganoglu's correlations give a much better agreement

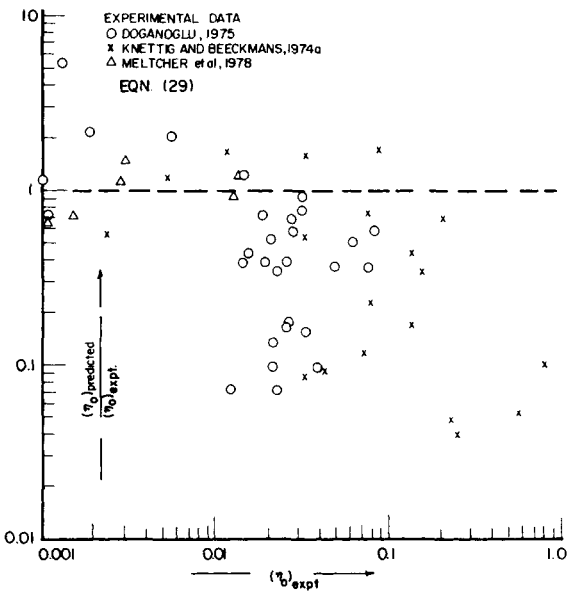

Figure 5. Comparison of experimental data with correlation by Paretsky (1972).

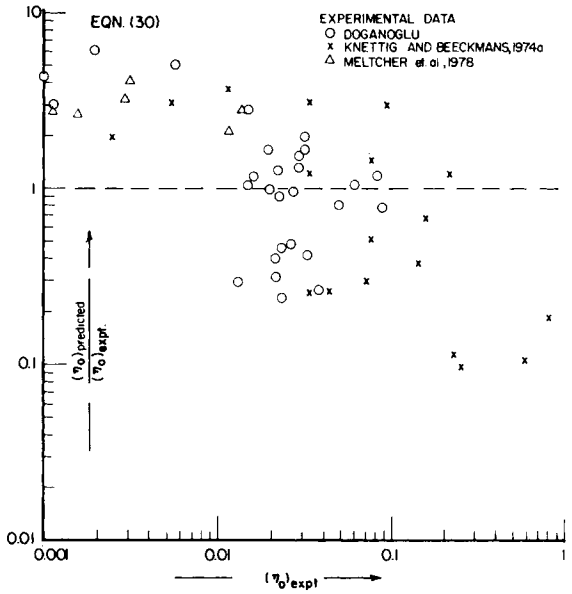

Figure 6. Comparison of experimental data with correlation by Meisen and Mathur (1974).

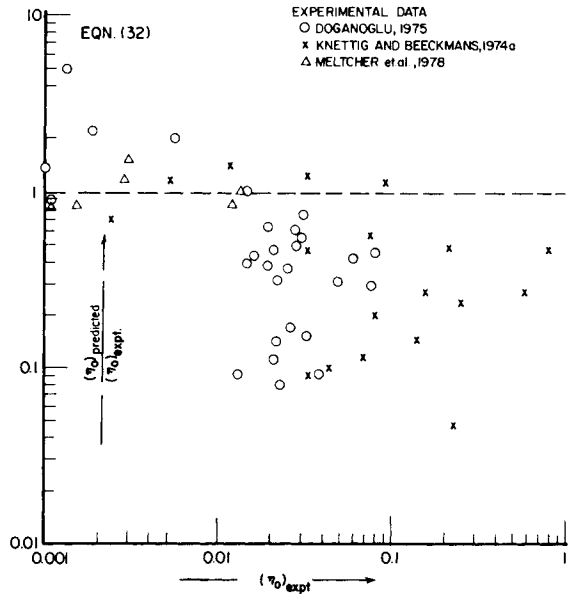

Figure 7. Comparison of experimental data with correlation by Meltcher et al. (1978).

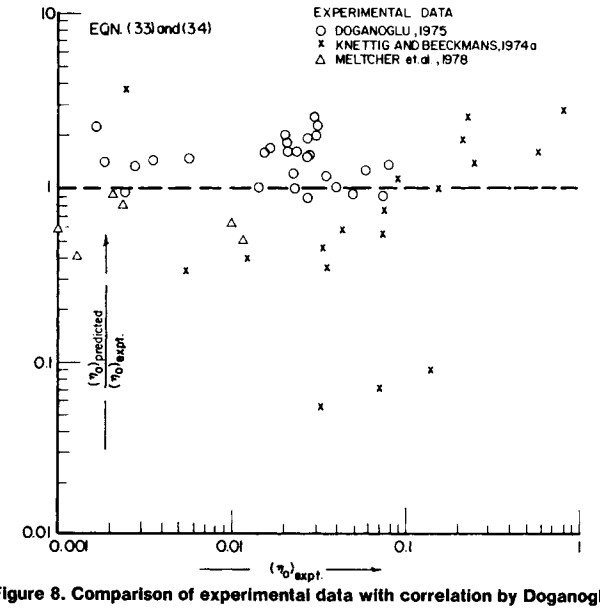

Figure 8. Comparison of experimental data with correlation by Doganoglu (1975).

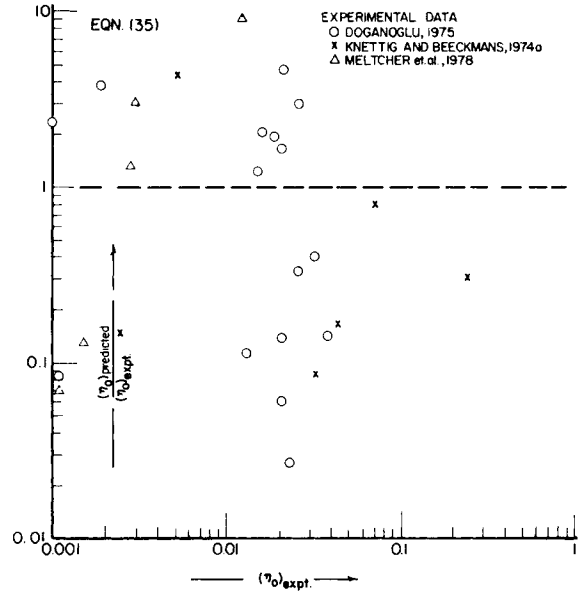

Figure 9. Comparison of experimental data with correlation by Thambimuthu et al. (1978).

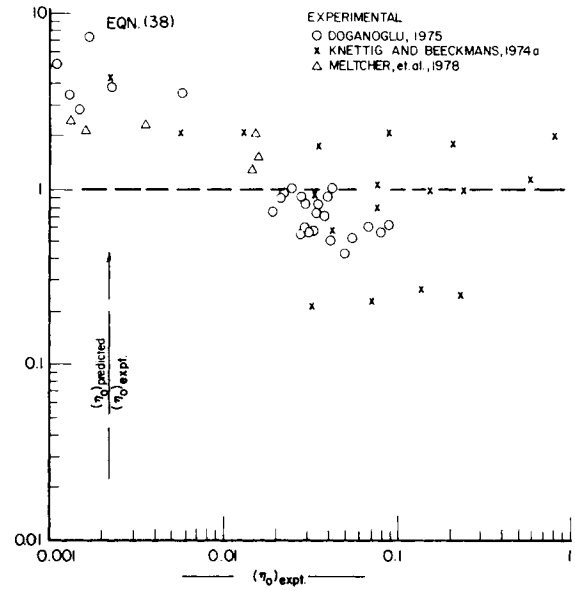

Figure 10. Comparison of experimental data with present correlation.

with his own data than with data reported by other investigators. This is not surprising since the correlations were obtained based on his data. Equation 38 does not display this bias. Second, Doganoglu's correlation, in fact, comprises two expressions; one for small grains ($d_c = 100\ \mu m$) and one for large grains ($d_c = 600\ \mu m$). The use of a dimensional variable (grain diameter) in a dimensionless correlation is an inconsistency. More importantly, there is the ambiguity as to which expression should be used if the filter grain is not equal to either of these two values.

Perhaps it should be emphasized that all the earlier correlations were obtained from regression analyses of experimental data. The inherent complexities of the experimental work necessarily limits the scope and ranges of the dimensionless parameters to be covered. Thus, none of the correlation includes all the known relevant dimensionless parameters. In contrast, Eq. 38 was established based on trajectory calculation results. Part of the the relationship was obtained analytically (i.e., Eq. 12) while other were derived from approximate expressions of numerical results. The dependence of (η_0) on each dimensionless group was established in a sequential manner. The only empiricism is in the manner in which the two tube configurations were combined. This particular approach used in establishing Eq. 38, to the authors' knoweldge, has not been at-

TABLE 4. ERROR PROPOGATION IN CALCULATION OF EXPERIMENTAL COLLECTION EFFICIENCY

	Error in Concentration Measurement, Relative to Feed Conc.								
	±1%			±5%			±10%		
C_{in}		100			100			100	
C_{in}^{+}		101			105			110	
C_{in}^{-}		99			95			90	
C_{out}	80	50	20	80	50	20	80	50	20
C_{out}^{+}	81	51	21	85	55	25	90	60	30
C_{out}^{-}	79	49	19	75	45	15	70	40	10
$C_{out}/C_{in})$	0.800	0.500	0.200	0.800	0.500	0.200	0.800	0.500	0.200
$C_{out}/C_{in})^{+}$	0.818	0.515	0.212	0.895	0.579	0.263	1.00	0.667	0.333
$C_{out}/C_{in})^{-}$	0.782	0.485	0.188	0.714	0.429	0.143	0.636	0.364	0.091
$-\ln(C_{out}/C_{in})$	0.223	0.693	1.609	0.223	0.693	1.609	0.223	0.693	1.609
$[-\ln(C_{out}/C_{in})]^{+}$	0.246	0.724	1.671	0.337	0.846	1.945	0.000	0.405	1.100
$[-\ln(C_{out}/C_{in})]^{-}$	0.201	0.664	1.551	0.111	0.546	1.336	0.453	1.011	2.397
$\left(\frac{\lambda_0^{+}}{\lambda_0}\right)$ or $\left(\frac{\eta_0^{+}}{\eta_0}\right)$	1.10	1.04	1.04	1.51	1.22	1.21	2.03	1.45	1.50
$\left(\frac{\lambda_0^{-}}{\lambda_0}\right)$ or $\left(\frac{\eta^{-}}{\eta_0}\right)$	0.9	0.96	0.96	0.50	0.79	0.83	0.00	0.58	0.68

Superscripts $^{+}$ and $^{-}$ denote the upper and lower limits of uncertainty, respectively.

tempted before. It does appear to offer certain advantages and conveniences, especially when it is difficult to obtain a large amount of accurate data over wide ranges of variables due to experimental difficulties. This is the situation in experiments of aerosol filtration in granular beds.

The correlation established predicts the initial collection efficiency, in most cases, within a factor of two of the experimental data (Figure 10). The comparison however should be viewed in light of the accuracy of the experimental data. The evaluation of the initial collection efficiency of granular filter beds is usually made from the knowledge of the influent and effluent particle concentration (c_{in} and c_{eff}) (Eq. 4), during the initial period of filtration. For low values of η_0 (i.e., $\eta_0 \ll 1$), Eq. 4 states that

$$\eta_0 = \text{constant} \cdot \left[-\ln \frac{c_{eff}}{c_{in}}\right] \tag{42}$$

An error propogation in the calculation of η_0 from values of influent and effluent concentrations is presented in Table 4, assuming different accuracy in particle concentration determinations. It is seen that an error of 1% (based on influent concentration) results in a 10% uncertainty in the value of η. Assuming that the accuracy of the concentration determination is 10% (which represents the capability of most common concentration determination instruments) the initial collection efficiency can only be determined within a factor of two or three. In view of this consideration, the agreement as shown in Figure 10 must be regarded as satisfactory.

Although the present correlation is more general and represents considerable improvement over previously established correlations, it should not be considered as definitive. The correlation requires further and more extensive testing against experiments. For this purpose, more accurate data on aerosol filtration in granular beds are urgently needed. It should also be mentioned that in the development of the correlation of this study, it is assumed that particle deposition occurs once a particle makes contact with the collector and the possibility of particles bouncing upon contact is ignored. Particle bouncing is known to be important in fibrous filtration (Loffler, 1979). Since the packing density of granular beds is much greater than that of fibrous beds, the likelihood of particles bouncing off is expected to be less in granular bed. It is however not clear whether this bouncing-off effect can be completely ignored, especially when the bed becomes substantially clogged. This is another area of study which merits the attention of future investigators.

ACKNOWLEDGMENT

This study was performed under Contract No. DE-AC02-79 ER 10386, Department of Energy.

NOTATION

A_s = parameter defined as $2(1-p^5)/w$; $p = (1-\epsilon)^{2/3}$ and $w = 2 - 3p + 3p^5 - 2p^6$
c_{in}, c_{eff} = influent and effluent particle concentrations
c_s = Cunningham's slip factor
d_c = constriction diameter of constricted tube
d_c^* = d_c/d_g
d_g = grain diameter
d_m = maximum diameter (entrance and exit) of constricted tube type unit cell
E = overall collection efficiency (Eq. 1)
h = height of unit cell
l = length of unit bed element, or center to center distance between two spheres
L = filter height
N_c = number of constriction per unit bed cross sectional area
N_G = gravity parameter, $2a_p^2(\rho_p - \rho_f)gc_s/9\mu V_s)$
N_G' = $2a_p^2(\rho_p - \rho_f)gc_s/9_\mu v_0)$
N_{Pe} = Peclet number $d_g V_s/D_{BM}$:D_{BM} Brownian diffusivity
N_R = relative size parameter, d_p/d_g
$N_{Re,s}$ = Reynolds number, $(d_g V_s \rho)/\mu$
N_{St} = Stokes' Number, $4a_p^2 V_s \rho_p C_s/9\mu d_g$
N_{St}' = $(4a_p^2\rho_p v_0 c_s)/9\mu h$
q = volumetric flow rate through a given unit cell
r = radial coordinate
r^* = r/h
r_e = radial coordinate of a particle at tube entrance, when it touches the tube wall
r_l = radial coordinate of the limiting trajectory
r_w = wall radius
t^* = tv_0/h
u_t = terminal velocity of particle
v_0 = mean velocity at throat section of constricted tube, $q/\pi r_0^2$
v_r = radial component of velocity
v_z = axial velocity component
V_s = superficial velocity
z = axial distance, bed depth
z^* = z/h

Greek Letters

ϵ = bed porosity
ψ = stream function
ψ^* = normalized stream function
η = initial collector efficiency of unit bed element

$(\eta)_c$ = collection efficiency of unit cell
$(\eta_0)_I$ = initial collection efficiency contribution due to interception
$(\eta_0)_i$ = initial collection efficiency contribution due to particle inertia
$(\eta_0)_D$ = initial collection efficiency due to Brownian diffusion
$(\eta_0)_G$ = initial collection efficiency due to gravitation
μ = fluid viscosity
ρ_f = fluid density
ρ_p = particle density

Subscripts

D = diffusion
expt = experimental
G = gravity
i = particle inertia
I = interception

LITERATURE CITED

Chiang, H. W., and Chi Tien, "Deposition of Brownian Particles in Packed Beds," to be published in *Chem. Eng. Sci.*

Chow, J. C. F., and K. Soda, "Laminar Flow in Tubes with Constriction," *Phys. Fluids*, **15**, 1700 (1972).

Doganoglu, Y., "Aerosol Collection in Fixed and Fluidized Beds," Ph.D. Dissertation, McGill University (1975).

Fedkiw, P., and J. Newman, "Mass Transfer at High Peclet Numbers for Creeping Flow in a Packed Bed Reactor," *AIChE J.*, **23**, 255 (1977).

Gutfinger, C., and G. Tadros, "Theoretical and Experimental Investigation of Granular Bed Dust Filters," *Atmos. Environ.*, **13**, 853 (1979).

Juvinall, R. A., R. W. Kessie, and M. J. Steindler, "Sand-Bed Filtration of Aerosols: A Review of Published Information on Their Use in Industrial and Atomic Facilities," ANL-7683, Argonne National Laboratory (1970).

Knettig, P., and J. M. Beeckmans, "Capture of Monodispersed Aerosol Particles in a Fixed and in a Fluidized Bed," *Canadian J. of Chem. Engrg.*, **52**, 703 (1974a).

———, "Inertial Capture of Aerosol Particles by Swarms of Accelerating Spheres," *J. Aerosol Sci.*, **5**, 225 (1974b).

Loffler, R., "Problems and Recent Advances in Aerosol Filtration," Symposium on Separation Science and Technology for Energy Applications, Department of Energy and Oak Ridge National Laboratory, Gatlinburg, TN (Oct., 1979).

Meisen, A., and K.B. Mathur, "The Spouted Bed Aerosol Collection: A Novel Device for Separating Small Particles from Gases," *Multiphase Flow Systems*, Inst. of Chem. Eng., Sym. Ser. 38, Paper K3 1974.

Meltcher, J. R., J. C. Alexander and Karim Zahedi, "Electrofluidizied Beds in the Control of Fly Ash," Final Report to Empire State Electric Energy Research Corp., 89 (Jan., 1978).

Neira, M. A., and A. C. Payatakes, "Collocation Solution of Creeping Newtonian Flow Through Periodically Constricted Tubes with Piecewise Continuous Wall Profile," *AIChE J.*, **24**, 43 (1978).

Paretsky, L. C., "Filtration of Aerosols by Granular Beds," Ph.D. Dissertation, The City University of New York, New York (1972).

Paretsky, L. C., L. Theodore, R., Pfeffer and A. M. Squires, "Panel Bed Filters for Simultaneous Removal of Fly Ash and Sulfur Dioxide Part II. Filtration of Dilute Aerosols by Sand Beds," *J. Air Pollution Control Assoc.*, **21**, 204 (1971).

Payatakes, A. C., Chi Tien and R. M. Turian, "A New Model for Granular Porous Media: Part I. Model Formulation," *AIChE J.*, **19**, 58 (1973a).

Pendse, H., "A Study of Certain Problems Concerning Deep Bed Filtration," Ph.D. Dissertation, Syracuse University, Syracuse, NY (1979).

Pendse, H., R. M. Turian and Chi Tien, "Deposition of Aerosol Particles in Granular Filter Bed," Symposium on Deposition and Filtration of Particles from Gases and Liquids, Society of Chemical Industry, London 95 (1978).

Rajagopalan, R., and Chi Tien, "Trajectory Analysis of Deep Bed Filtration Using the Sphere-in-Cell Porous Media Model," *AIChE J.*, **22**, 523 (1976).

Tardos, G. I., N. Abuef, and C. Gutfinger, "Diffusional Filtration of Dust in a Fluidized Bed," *Atmos. Environ.* **10**, 389 (1976).

Tardos, G. I., N. Abuaf, and C. Gutfinger, "Dust Deposition in Granular Filter Bed Filters: Theories and Experiments," *J. Air. Poll. Control Assoc.*, **28**, 354 (1978).

Tardos, G. I., E. Yu, R. Pfeffer, and A. M. Squires, "Experiments on Aerosol Filtration in Granular Sand Beds," *J. Colloid. Interface Sci.*, **71**, 616 (1979).

Thambimuthu, K. V., Y. Doganoglu, T. Farrokhalaee, and R. Flift, "Aerosol Filtration in Fixed Granular Beds," Symposium of Deposition and Filtration of Particles from Gases and Liquids, Society of Chemical Industry, London, 107 (1978).

Venkatesan, M., and R. Rajagopalan, "A Hyperboloidal Constricted Tube Model of Porous Media," *AICHE J.*, **26**, 694 (1980).

Manuscript received October 8, 1980; revision received September 23, and accepted October 13, 1981.

Decomposition Strategy for Designing Flexible Chemical Plants

I. E. GROSSMANN and K. P. HALEMANE

Department of Chemical Engineering
Carnegie-Mellon University
Pittsburgh, PA 15213

One of the main computational problems faced in the optimal design of flexible chemical plants with multi-period operation is the large number of decision variables that are involved in the corresponding nonlinear programming formulation. To overcome this difficulty, a decomposition technique based on a projection-restriction strategy is suggested to exploit the block-diagonal structure in the constraints. Successful application of this strategy requires an efficient method to find an initial feasible point, and the extension of current equation ordering algorithms for adding systematically inequality constraints that become active. General trends in the performance of the proposed decomposition technique are presented through an example.

SCOPE

Flexibility in chemical plants is normally introduced in practice by applying empirical overdesign factors to sizes of equipment that have been designed for a nominal operating condition. This procedure is clearly not very satisfactory as it has little rational basis. For instance, with empirical overdesign it is unclear what range of specifications the overdesigned plant

Correspondence concerning this paper should be addressed to I. E. Grossman.